Computational analysis of the high-pressure structures of InSb

2000 J. Phys.: Condens. Matter 12 7161

(http://iopscience.iop.org/0953-8984/12/32/301)

J. Phys.: Condens. Matter **12** (2000) 7161–7173. Printed in the UK PII: S0953-8984(00)13726-9

Computational analysis of the high-pressure structures of InSb

A A Kelsey and G J Ackland

Department of Physics and Astronomy, The University of Edinburgh, Edinburgh EH9 3JZ, UK

Received 4 May 2000, in final form 23 June 2000

Abstract. We present results of pseudopotential calculations for the high-pressure phases of indium antimonide, showing that the recently observed *Cmcm* superlattice structure is the most stable crystal structure at high pressure. Furthermore, we show that the competing high-pressure phases observed in this and other III–V semiconductors can be characterized into a hierarchy by ordering and topology and that symmetry is a secondary characteristic in determining the energy.

1. Introduction

There has been a huge upsurge in interest in the high-pressure structure of the tetrahedral semiconductors recently, due to the development of two new techniques: diamond anvil cells allied to the image plate x-ray detector and the pseudopotential implementation of the density functional theory combined with the availability of fast computers [1]. Spectacular agreement has been observed between the two methods, with experimental results showing small distortions from the simple structures which had been suggested by early workers, and calculation now able to determine which observed phases are stable and which metastable—and also to predict stable phases which might not have been observed due to transition kinetics.

By virtue of its series of phase transitions, and exceptionally sharp high-pressure diffraction patterns, indium antimonide has been among the most heavily studied materials. InSb has the zinc-blende structure at ambient pressure, but the detailed high-pressure systematics were only revealed in 1993 with image plate analysis [2] and extremely careful x-ray diffraction study, uncovering one of the most complicated high-pressure crystal structures yet solved, a 12-atom unit cell named the super-*Cmcm* phase to distinguish it from the simpler structure with the same symmetry found in GaAs [3].

The InSb equilibrium phase diagram is summarized in figure 1 following the notation of the recent comprehensive review by Nelmes and McMahon [1]. The experimental work is complicated by the appearance of metastable intermediate phases and the observed sequence of phases under increasing pressure at room temperature is as follows: the zinc-blende structure transforms to a mixture of disordered β-tin and *Immm* before transforming to a single phase of *Immm*. This phase then goes through a transition to the super-*Cmcm* structure. Work at higher pressure by Nelmes and McMahon has shown that the super-*Cmcm* structure transformed back to *Immm* at pressures above 10 GPa via an intermediate structure that they called P5†. The behaviour of the *Immm* phase at room temperature is particularly strange, appearing both as a metastable intermediary at low pressure and as a truly stable phase at higher pressure.

† The P5 (phase 5) notation simply indicates that the space group has yet to be fully characterized. Other (solved) phases are P1 (zinc-blende), P2 (β-tin), P3 (*Immm*), P4 (super-*Cmcm*).

0953-8984/00/327161+13$30.00

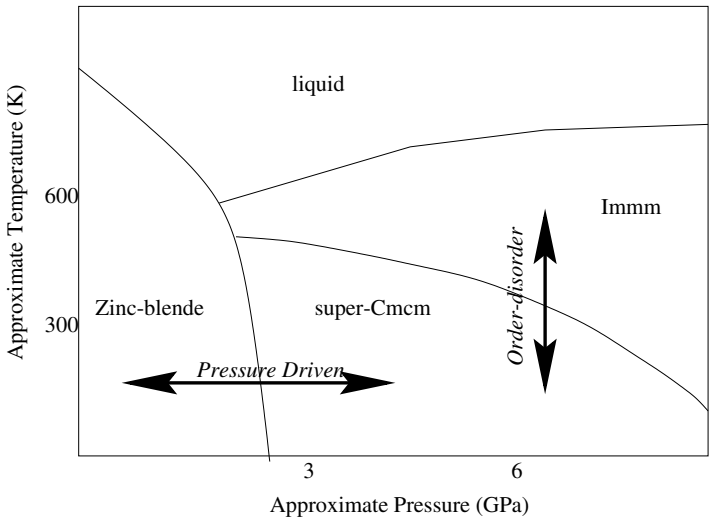

Figure 1. A schematic representation of the equilibrium temperature–pressure phase diagram of InSb from x-ray diffraction and the present calculations [1,26]. Zinc-blende is the cubic zinc-blende structure. Super-$Cmcm$ and $Immm$ are decorations of the simple hexagonal lattice described in the text. The experimental work [26] suggests a re-entrant behaviour of the $Immm$ phase but we can find no theoretical evidence for this. The figure omits the β-tin phase, the low-pressure $Immm$ phase and the high-pressure P5 phase which are predicted in this paper to be metastable. Temperatures given in the figure are intended as illustrative only and do not represent theoretical predictions.

At even higher pressures [5] ($\sim$17 GPa) $Immm$ again becomes unstable to an intermediate structure which ultimately transforms to a BCC phase. These structures will not be considered here and consequently are not shown in figure 1.

The naming of the phases can give rise to confusion. This is because the experimentally reported structures are actually the highest-symmetry phases consistent with the data: there is always the possibility that the weak diffraction peaks due to small symmetry-breaking distortions or medium-range ordering cannot be resolved. With improvements in experimental technique better resolution has led to the reporting of phases of ever lower symmetry, and now the ability to determine the absence of weak peaks gives confidence that the true space group has been determined.

Here, we group the $Immm$, $Cmcm$ and super-$Cmcm$ phases together as 'simple hexagonal analogues'. This is appropriate because these are the symmetries which arise from simple binary ordering on a simple hexagonal lattice. Likewise, we will consider different ordering on an underlying β-tin lattice, and associated symmetry breaking.

In this paper we address a number of issues regarding the InSb phase diagram based on total-energy calculations of the observed structures and others which could be expected to be competitive based on their existence in other tetrahedral semiconductors. Using these results we also address the observation of disordered phases at room temperature and the appearance of metastable intermediates. The paper is arranged as follows. In section 2 we discuss the possible crystal structures which we will be considering, then in section 3 the total-energy calculations are presented. Since these calculations are at zero kelvin, models for the high-temperature behaviour are introduced in sections 4 and 5 to cover both order–disorder and soft-phonon-type temperature-induced transitions. Finally we draw conclusions and present a theoretical interpretation of the (meta)stability of the observed phases.

2. General structural considerations

The high-pressure phases in binary III–V semiconductors [1] can generally be related to those of silicon: diamond, β-tin†, simple hexagonal and the metastable distorted fourfold-coordinated BC8 structure. Other phases observed experimentally, such as cinnabar [6], have been shown to be metastable [3]. Forming a binary equivalent of these covalent structures is straightforward when one recognizes that most compounds have secondary ionic bonding, which favours unlike nearest-neighbour atoms. Thus the zinc-blende, SC16 and rock-salt‡ structures have a unique ordering making all nearest neighbours unlike, and all have been observed at high pressure in III–V compounds. By contrast, structures with odd-membered rings, for which such orderings are impossible, such as Si-XII (R8) [7], have high energy [8] and are not observed. For InSb previous calculations have demonstrated the relative stability of these phases, showing that neither SC16, rock-salt nor any ordering of R8 is stable [4, 9]. These structures are described in a number of recent reviews [1, 4].

In this section we consider possible binary decorations of the simple hexagonal and β-tin structures based on the premise that the energy is determined by the number of unlike neighbours.

2.1. Simple hexagonal analogues

For the simple hexagonal structure, it is impossible for all six neighbours of every atom in the close-packed layer to be of the opposite species. The most unlike neighbours that can be achieved in a periodically repeating structure is four, and there are infinitely many ways of achieving this. The three experimentally observed patterns, $Immm$, $Cmcm$ and super-$Cmcm$, are shown in figures 2(a), 2(b), 2(c): the perpendicular continuation of the hexagonal layers is a columnar alternation of black and white atoms§.

It is actually possible to obtain more than four unlike neighbours per atom in an aperiodic structure, as shown in figure 2(d). The special axis here might be viewed as a nucleation site for ordering from the disordered phase, but forming boundaries between domains of this type would at best return the mean number of unlike neighbours to four‖.

As shown in figure 3 it is possible to maintain hexagonal symmetry with a maximal-unlike-neighbour decoration of the hexagonal lattice, although there is no experimental evidence for its existence¶.

Of the three structures which have been observed experimentally, the simplest is $Immm$ which has alternate parallel stripes, then the zigzag structure of the $Cmcm$ and finally the larger zigzags of the super-$Cmcm$. Ignoring small distortions from the simple hexagonal sites, and considering the structures in terms of bonding hierarchy, there is no obvious difference in packing efficiency or covalent bonding (each has eight neighbours). Ionic bonding gives very similar Madelung constants for each structure (dominated by the six unlike neighbours). Thus there is likely to be a delicate balance of energies between these structures: indeed it has been established from *ab initio* calculation in GaAs that more subtle electronic effects lead to

† Strictly, the crystal structure originally identified as the β-tin phase in silicon is slightly orthorhombically distorted to $Imma$, the monatomic equivalent of $Imm2$.

‡ These are the binary analogues of the diamond, BC8 and simple cubic structures.

§ Although we think of these structures as based on the simple hexagonal lattice, they do not actually have simple hexagonal symmetry.

‖ If this is the most favoured atomistic nucleation site, since it gives rise to an aperiodic structure, it is likely that the ordering process will be slow.

¶ To generate such a hexagonal structure based on preferred nucleation sites rather than overall stability would require that the ordering nuclei were distributed on a superlattice.

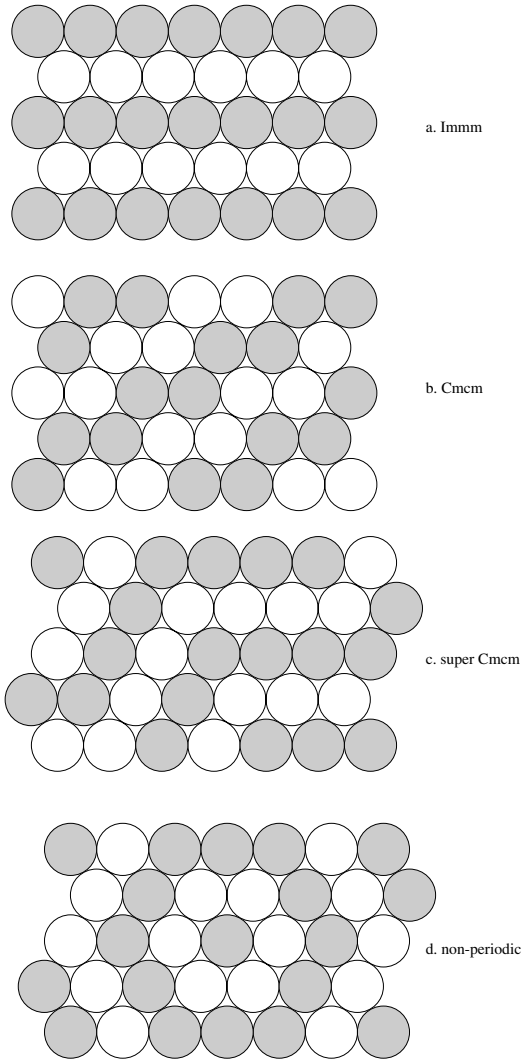

Figure 2. Possible decorations of a simple hexagonal lattice giving rise to (a) $Immm$, (b) $Cmcm$ and (c) super-$Cmcm$ structures (atom types alternate in subsequent layers), and (d) a non-periodic structure which has more than four unlike neighbours.

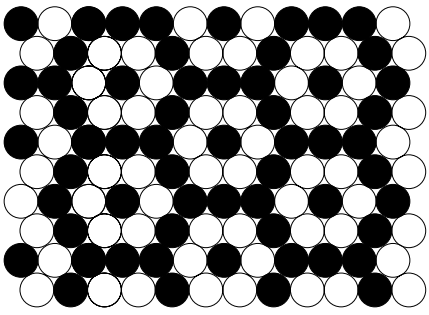

Figure 3. Hexagonal decoration of a hexagonal lattice showing the possibility of atoms with six unlike near neighbours forming part of a crystalline structure

Cmcm having lower energy [3].

It is notable that the breaking of simple hexagonal symmetry by these structures is fully determined by the location of the atoms on the sites of the hexagonal lattice. Although in the experimentally reported structures the atoms are slightly displaced from ideal hexagonal sites, these displacements do not break any further symmetry. For this reason we categorize them as hexagonal decorations rather than as stackings of NaCl planes [1].

2.2. β-tin analogues

The binary equivalent of the β-tin structure is straightforward if one considers it to be a fourfold-coordinated structure (the bonding topology and the anion/cation ordering are then identical to those of zinc-blende). However, the pair of neighbouring atoms along the *c*-axis are very close to being near neighbours. If one treats β-tin as sixfold coordinated then there are five-membered rings and no unique structure which maximizes the number of unlike near neighbours. Furthermore, the 'zinc-blende' ordering is then not even one of the structures which maximizes the number of unlike near neighbours.

No ordered β-tin-like phase has been reported experimentally [10].

At some pressures, the β-tin structure of silicon is unstable with respect to a small distortion to $Imma$. The equivalent distortion in a binary compound would give rise to the $Imm2$ structure (figure 4). This structure can be regarded as a small distortion from either β-tin or $Immm$. It has been suggested as a possible stable phase of InSb [11], and although the experimental data at room temperature rule it out, it is conceivable that it could exist at low temperatures.

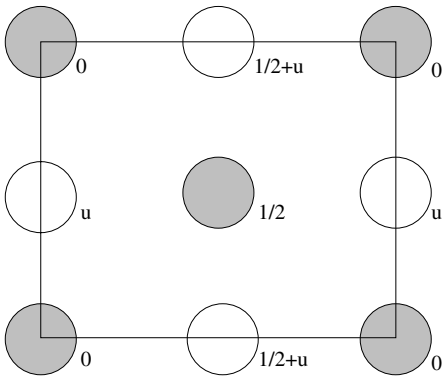

Figure 4. A projection drawing of the body-centred orthorhombic $Imm2$ structure viewed down the *c*-axis. Grey and white circles represent atoms of different species. Special cases of this include $Immm$ ($u = 0.5$), NaCl ($u = 0.5$ and $a = c = b/\sqrt{2}$), β-tin ($a = b$, $u = 0.25$) and zinc-blende ($a = b = \sqrt{2}c$, $u = 0.25$).

3. Zero-temperature *ab initio* simulations

A number of previous papers have described *ab initio* total-energy calculations using the density functional [12, 13] plane-wave pseudopotential method [14] for III–V materials at pressure [3, 9, 15–18]. Here we report the results of similar calculations for InSb.

We have calculated total energies for the following structures: zinc-blende, ordered β-tin, a model for disordered β-tin, $Immm$, $Imm2$, SC16, rock-salt, $Cmcm$ and the super-$Cmcm$ phase (see figures 2–4). For all the structures considered all degrees of freedom were relaxed

(electrons, ionic coordinates and the shape and size of the cell).

The plane-wave expansion was truncated at terms with a kinetic energy of 300 eV. This was found to converge the total energies to better than 0.1 meV per atom. The reciprocal-space sampling was performed using the symmetry-reduced sets of Monkhorst and Pack [19]. The sets used were as follows. The semiconducting zinc-blende phase was sampled with a $6 \times 6 \times 6$ set. The metallic inversion domain boundary (IDB) structure, described in section 5 below, the β-tin phase, the $Imm2$ phase and the $Immm$ phase used $10 \times 10 \times 8$, $10 \times 10 \times 14$, $12 \times 12 \times 20$ and $10 \times 10 \times 16$ sets respectively. For the rock-salt phase an $11 \times 11 \times 11$ set was found to be sufficient to converge the total energy to better than 0.1 meV per atom. The numbers of special k-points used was then 300 for the $Imm2$ phase, 200 for the $Immm$ phase, 296 for the β-tin phase and 100 for the IDB structure. The semimetallic SC16 phase and the super-$Cmcm$ phase both only required a $4 \times 4 \times 4$ grid to give a similar level of k-point convergence at 5 meV per atom. Previous work has shown that including the 4d states either explicitly [11] or via non-linear core corrections [16] can be important: we use the ultrasoft-pseudopotential scheme [20] and include the 4d states as valence electrons in our calculations.

In each case the internal and lattice parameters were optimized by evaluation of *ab initio* stresses and Hellmann–Feynman forces: the atoms were moved until the forces fell to zero and the lattice parameters altered until the residual stresses were hydrostatic [21]. The results of these calculations are given in figure 5.

For the three 'simple hexagonal' structures, even this level of convergence was insufficient to convincingly distinguish their energies [8]. Consequently we adopted a different strategy to

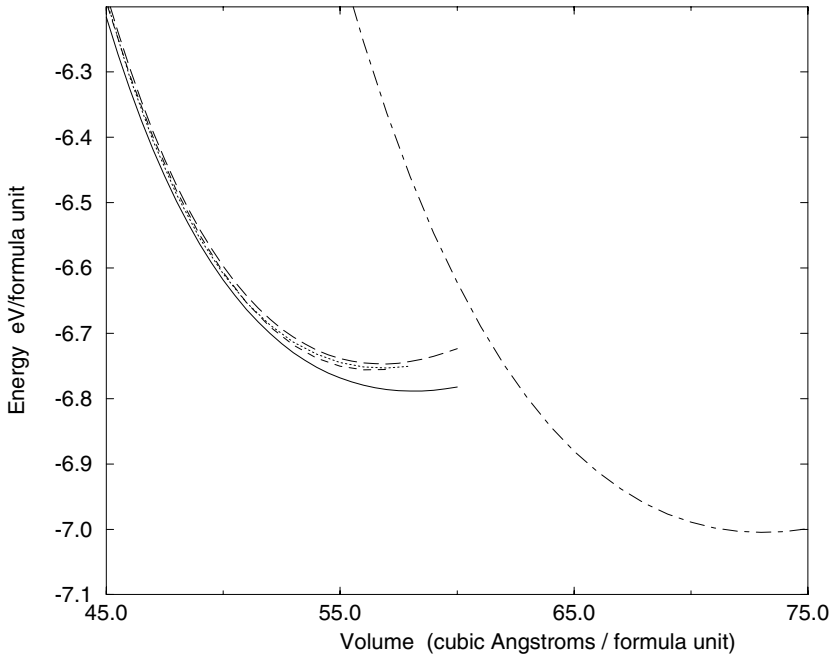

Figure 5. Energy versus volume for all the InSb phases considered. Curves are fits to about 20 data points using the Birch–Murnaghan equation of state. The zero of energy was taken as the isolated atoms. The solid line represents super-$Cmcm$, the dotted line β-tin, the short-dashed line $Immm$, the long-dashed line $Cmcm$ and the dot–dashed line zinc-blende. The phase transition from zinc-blende to super-$Cmcm$ is determined from the common-tangent construction to be 2.3 GPa, in excellent agreement with the 2.1 GPa reported experimentally.

examine directly the energy differences between the three phases. An equivalent monoclinic supercell was used to describe each pair of phases: 12 atoms for super-$Cmcm$ versus $Cmcm$, 4 atoms for $Cmcm$ versus $Immm$. Direct comparison of super-$Cmcm$ with $Immm$ in an equivalent cell would require 24 atoms and was not done. Identical k-point sets ($4 \times 4 \times 4$ and $10 \times 10 \times 8$) were employed for each which gives rise to cancellation of sampling errors and means energy differences are better converged.

The energy comparison between the three 'simple hexagonal' structures is shown in figure 6. The most complex structure, the super-$Cmcm$, can be seen to have very slightly the lowest energy. Curiously, it also has the largest equilibrium volume, and (marginally) the largest volume at each pressure. This is consistent with the experimental observation that the super-$Cmcm$ which appears on recrystallization is slightly less dense than the intermediate $Immm$.

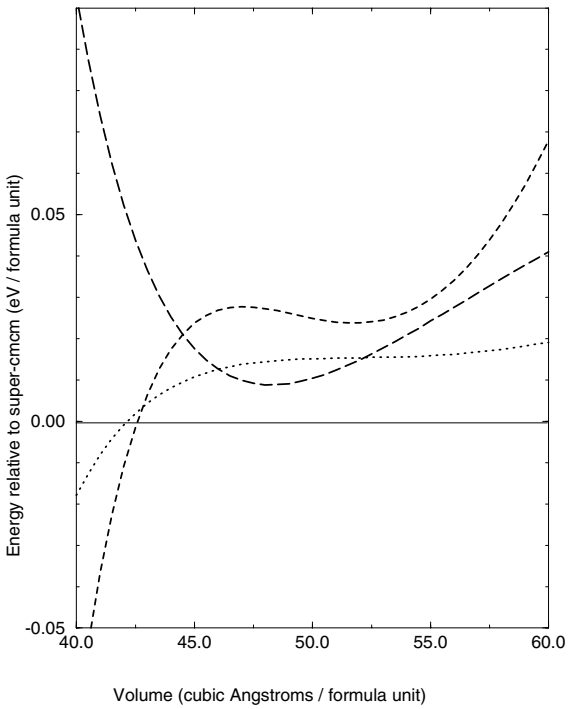

Figure 6. Energy relative to the super-$Cmcm$ structure versus volume using k-point matching for the hexagonal decorated InSb phases considered and for the ordered β-tin phase. The dotted line represents β-tin, the short-dashed line $Immm$ and the long-dashed line $Cmcm$. The lines are differences between fits to about 20 data points using the Birch–Murnaghan equation of state. We have no explanation for oscillations in the curves which may be due to noise. Notice the extremely small scale of the y-axis.

The results suggest a 0 K pressure-induced transition from zinc-blende to super-$Cmcm$ at 2.4 GPa, in good agreement with experiment. They also imply a transition from super-$Cmcm$ to $Immm$ at 26 GPa, qualitatively correct but above the observed room temperature value. This may arise from the strong temperature dependence of this transition pressure [1] illustrated in figure 1.

The β-tin structure was also evaluated and found to be very close in energy to the simple hexagonal structures, but never stable.

These lattice parameters and internal parameters for all the phases calculated agree well with the experimental observations, and their values at 6 GPa are quoted in table 1 and compared with experimental data.

Table 1. Relaxed parameters for the InSb phases studied, taken from 6 GPa calculations. Experimentally measured values from Nelmes and McMahon [25] are given in brackets for comparison. With the exception of the volume, the parameters chosen for this table vary slowly with pressure.

Structure	Volume (Å^3)	c/a	b/a	In parameters	Sb parameters
Zinc-blende		1	1	—	—
β-tin	51.39	0.5404 (0.5448)	1	—	—
$Immm$	51.40	0.538 (0.544)	0.907 (0.921)	—	—
$Cmcm$	51.27	1.0482	0.929	$y = 0.7260$	$y = 0.2154$
Super-$Cmcm$	51.42	2.838 (2.872)	1.031 (1.050)	4(c): $y = 0.110$ (0.120)	$y = 0.606$ (0.620)
Super-$Cmcm$				8(f): $y = 0.413$ (0.411)	8(f): $y = 0.915$ (0.910)
Super-$Cmcm$				8(f): $z = 0.085$ (0.089)	8(f): $z = 0.079$ (0.081)

4. Soft modes in β-tin, $Immm$ and $Imm2$

Previous experimental [2] and theoretical work [11] has suggested the possibility that the $Immm$ phase might in fact have $Imm2$ symmetry. $Imm2$ can be related to $Immm$ and β-tin by a soft-phonon distortion, coupled to a lattice shear [1], as shown in figure 4. We have performed calculations along this pathway under two separate assumptions regarding boundary conditions.

Figure 7 shows the results of the calculations of the variation in enthalpy under constant pressure with fixed u relative to $Immm$. These calculations reveal structural stability under hydrostatic conditions. Consistent with figure 6, the β-tin phase is favoured at low pressures and the $Immm$ at high pressure. Both structures lie at minima of the enthalpy and are metastable; however, there is no region of $Imm2$ metastability.

Figure 8 shows the results of the calculations of the variation in energy under constant volume with a range of unrelaxed u; the lattice parameters are taken from the $Immm$ or β-tin structures. These 'frozen-phonon' calculations represent the structures accessible to vibrations of the Γ-point optic phonon. The metastability of the $Immm$ structure is again clear, as is the fact that coupling of the internal coordinate to the strain is needed to transform to β-tin.

In the β-tin phonon calculation (dashed line), the $u = 0$ structure can be regarded as a barrier between one β-tin structure and an equivalent. At 6 GPa this barrier is only 0.026 eV per atom, making it possible that the columns of like-species atoms could slide relative to one another along the c-axis, assisting rapid atomic diffusion. This may contribute to the broad diffraction peaks reported for the β-tin structure.

Energy comparisons between $Imm2$, $Immm$ and β-tin at zero temperature and low hydrostatic pressure show that β-tin is more stable, but the energies of all three are very close. At high pressure $Immm$ becomes more stable. We find no evidence for the stability of $Imm2$ under hydrostatic conditions†: although the energy associated with the soft-mode

† As far as we can determine, $Imm2$ is not even metastable since the energy increases as u is varied from 0.5 (see figure 4) even if the lattice parameters are allowed to relax. For small deviations from 0.5 the restoring forces in $Imm2$ are below the convergence criteria adopted in other calculations. Unlike $Immm$, $Cmcm$ etc the $Imm2$ structure does involve more symmetry breaking from simple hexagonal than is entailed by ordering of the anions and cations.

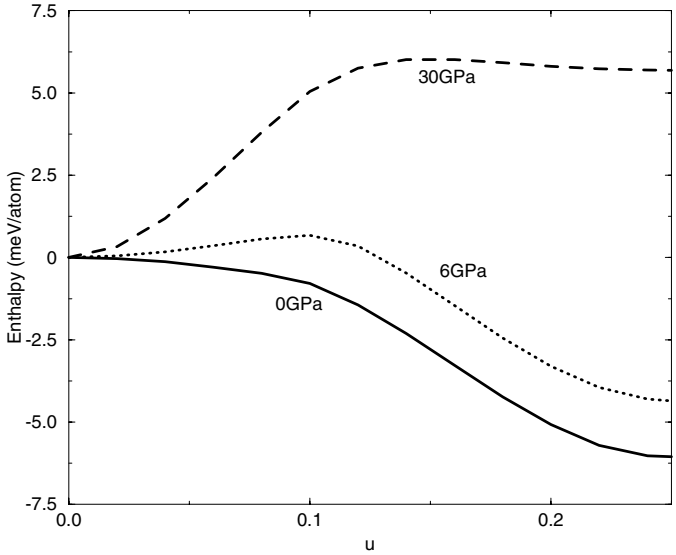

Figure 7. Relative enthalpy versus internal parameter u for $Imm2$ structures at a three different pressures. The end points of the graph $u = 0$ and $u = 0.25$ represent $Immm$ and β-tin symmetry respectively.

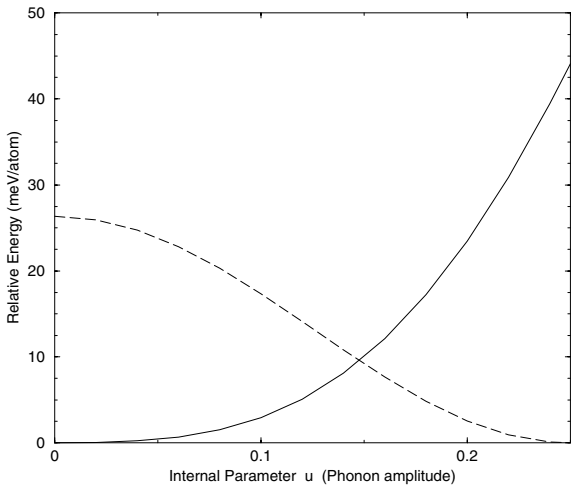

Figure 8. Relative energy versus internal parameter u for Γ-point 'frozen'-phonon calculations for β-tin (dashed line) and $Immm$ (solid line). The unit cells correspond to the 6 GPa equilibrium structures.

distortion (which corresponds to a low-frequency Γ-point mode in $Immm$) is small, it never becomes negative. If a non-hydrostatic pressure† is applied, either of the $Immm$ and $Imm2$ structures can be stabilized. This is consistent with previous work which found zero energy

† Computationally, this means the external stress σ_{yy} along the b-direction is set different to that along the a-direction. The total energy plus $(\sigma_{xx}a + \sigma_{yy}b + \sigma_{zz}c)$ is then minimized with respect to the internal degrees of freedom and the lattice parameters. Previous workers [11] were unable to relax all degrees of freedom simultaneously and hence could not determine the correct hydrostatic structure.

difference (to within calculational accuracy) between $Imm2$ and $Immm$ [11] in calculations for which the stress was not hydrostatic.

Since $Imm2$ is the lower-symmetry phase (in a Landau picture) its calculated mechanical instability implies thermodynamic instability at all temperatures.

Note that the $Immm$ and β-tin phases are both metastable with respect to super-$Cmcm$.

5. Site disorder in β-tin

Disorder in InSb was previously investigated with respect to formation of inversion domain boundaries (IDB) as an explanation for the lack of difference peaks for depressurized zinc-blende and $Immm$. The diffraction pattern of the β-tin phase differs in character from that of the other phases of InSb in that the diffraction peaks are broader and the strongest 'difference' peak (from In–Sb out-of-phase scattering) is absent [1]. The traditional interpretation of this absence is that the phase is disordered. However, both these effects (peak broadening and the lack of the difference peak) can be explained by the presence of IDBs. An IDB does not disrupt the arrangement of sites but swaps the atomic species†. In previous work the (110) IDB in zinc-blende InSb was found to have an energy of 0.285 eV per pair of like-species near neighbours ('wrong bond') [18].

We have performed a similar calculation on a cell which comprises a reordering of the atoms on the β-tin lattice increasing the number of unlike second neighbours along the c-direction at the cost of creating like-neighbour pairs. With respect to 'zinc-blende-ordered' β-tin (figure 4) it can be regarded as an IDB every fourth layer. It is also one of the structures which maximizes the number of first + second unlike neighbours.

By taking the difference between the total energies of the IDB structure and the β-tin phase, the energy per wrong bond can be calculated for the β-tin phase. This turns out to be 0.004 eV, significantly lower than the energy of a wrong bond in the zinc-blende phase. It is also worth noting that the energy of the wrong bond drops significantly between the relaxed and unrelaxed structures showing that, as in the zinc-blende case [18], ionic and cell relaxation are important in obtaining accurate energetics—however, in the real material full relaxation may not be possible, so our wrong-bond energy represents a lower bound.

6. Discussion

In much previous work comparing total-energy calculations with high-pressure experiment the effect of temperature has been ignored. The excellent results obtained suggest that the free-energy differences arising from effects such as zero-point motion and phonons seem to have little effect in determining stability at room temperature. The calculations here suggest two transitions between stable structures: zinc-blende $\rightarrow$ super-$Cmcm$ $\rightarrow$ $Immm$. This appears to be at variance with the experimentally reported β-tin and $Immm$.

A clue to the resolution of this comes from the diffraction patterns themselves: those of β-tin and $Immm$ are broader than those of zinc-blende or super-$Cmcm$, indicating that the crystals are either small or contain many defects. Both calculation and experiment agree that the super-$Cmcm$ phase is less dense at a given pressure than the β-tin and $Immm$. This is thermodynamically inconsistent with the transition from $Immm$ to super-$Cmcm$ on increasing pressure. A more likely interpretation is that super-$Cmcm$ is the stable phase, while the initial appearance of $Immm$ is merely a metastable structure.

† The two domains on either side of the IDB scatter coherently, but the contributions from each to the difference peaks are out of phase leading to a much reduced amplitude.

Using the wrong-bond energy it is possible to estimate the thermodynamic order–disorder temperature of β-tin InSb. Long-range order is destroyed when the number of wrong bonds exceeds the percolation threshold, which in this case is the same as for diamond—39% of bonds [18]. Assuming that in a general configuration relaxation is more difficult, we take the unrelaxed wrong-bond energy deduced from the IDB structure to obtain an energy difference of 0.008 eV/atom between ordered and disordered β-tin. This implies an order–disorder temperature well below room temperature: in the case of InSb using the simple theory of Bethe [22] gives an order–disorder transition at around 40 K. This explains the fact that observations of the β-tin phase in InSb (and III–V phases in general [10]) have always shown it to be disordered.

In the simple hexagonal-type structures wrong bonds in the c-direction are energetically very unfavoured. Thus disorder can occur only in the hexagonal plane. One can describe the experimentally reported periodic orderings as involving stripes with kinks: $Immm$ has no kinks, $Cmcm$ has kinks on every row and super-$Cmcm$ a kink in every third row (see figure 2).

A further possibility is that the stripes have randomly ordered kinks. Such a structure would be orthorhombic, $Immm$, with the mean direction of the stripes determining a unique axis and may be a candidate for the intermediate $Immm$ phase†. With time, this structure will anneal out to the most stable structure, which in the case of InSb is super-$Cmcm$. Note that although the energy differences between decorations are very small, the kinks only provide disorder in one dimension, and hence cannot contribute enough entropy to drive a temperature-driven order–disorder transition in the thermodynamic limit‡.

In the first phase transition it is likely that the disordered-kink structure could form quite rapidly, with the super-$Cmcm$ decoration of the close-packed plane evolving more slowly. This is consistent with the room temperature diffraction data, which initially show a metastable $Immm$ phase with broad peaks. This is followed by a growth of super-$Cmcm$ with very sharp peaks, showing that the defects anneal out.

At high pressures, the larger volume of super-$Cmcm$ makes it less stable than the ordered $Immm$ phase, so the nature of this transition is uncontroversial.

7. Conclusions

The sequence of observed phase transitions in InSb can be easily understood by comparison with silicon. The predominant bonding in each case is covalent, and the covalent frameworks of the observed structures are identical. In silicon the first three stable phases are diamond, β-tin (slightly distorted to $Imma$ at 0 K or higher pressure) and simple hexagonal. In InSb the first four observed structures are simply binary equivalents of the silicon ones: zinc-blende, β-tin, $Immm$ and super-$Cmcm$.

In InSb, unlike almost all the other III–V semiconductors [15–17], the SC16 phase is not predicted to be stable at any pressures. The theoretical sequence of low-temperature stable structures is simply zinc-blende to super-$Cmcm$ to $Immm$.

The complex and apparently diverse structural systematics in III–V semiconductors can be related to the absence of a unique binary simple hexagonal structure which maximizes numbers

† The 'disorder' proposed here is the one-dimensional ordering of the kinks in figure 2. If the lines of similar atoms do not form closed loops, there will be mirror planes parallel and perpendicular to the mean stripe direction and perfect order in the c-direction, giving overall $Immm$ symmetry. The disordering will give rise to broad diffraction peaks and the diffraction pattern from such a phase will appear to have $Immm$ symmetry. The ordering in planes perpendicular to the unique axis, combined with the ordering in the c-direction, underlies the alternate description of these phases in terms of NaCl layers.

‡ For N atoms the kink configurational entropy increases as $N^{1/3}$ while the energy difference increases as N. It is possible that for small crystallites $Immm$ will be stabilized over super-$Cmcm$ by such finite-size effects.

of unlike nearest neighbours. The observed structures, $Immm$, $Cmcm$ and super-$Cmcm$, all have symmetries corresponding exactly to different decorations of the simple hexagonal structure, and although the observed atomic positions are slightly displaced from the simple hexagonal lattice, these displacements do not in any case entail any symmetry breaking beyond that introduced by the ordering of the cations and anions. In all these structures the differences in order are confined to the hexagonal plane: hence a disordered combination of them will not have an extensive entropy. To disorder a simple hexagonal structure three dimensionally requires an increase in the number of unlike nearest-neighbour bonds.

The non-unique ordering of the β-tin structure, with the possibility of compensating for like-species near neighbours with unlike second neighbours, leads to a very low order–disorder transition temperature. Moreover, it is conceivable that a disordered β-tin phase, with higher configurational entropy than $Immm$, could have a region of stability at high pressure and temperature.

The internal coordinates and lattice parameters of the super-$Cmcm$ phase reported in InSb are very well reproduced in the calculation, and it is found to be the energetically favourable decoration of a hexagonal lattice over the simpler $Cmcm$ and $Immm$. At a given pressure, super-$Cmcm$ has a larger atomic volume than $Immm$ and hence $Immm$ has the lower enthalpy at high pressures.

There are a number of additional interesting features of the super-$Cmcm$ phase. It does not appear immediately on pressure increase, but rather after the sample is left for some time. Its growth can be accelerated by annealing even though higher temperatures take it toward the edge of its stability field, and by increased pressure even though it has a slightly larger volume than $Immm$. Finally, the diffraction pattern observed on an area detector is not a smooth ring, but has a 'spotty' appearance [2]. All this is evidence of large crystallite sizes arising from slow recrystallization kinetics, consistent with our calculated result that many competing metastable phases with very similar energy exist.

In sum, the results of our calculations and analysis reveal a theoretical interpretation fully consistent with the experimental pressure and temperature phase diagram. Moreover, the appearance of intermediary phases and order–disorder thermal transitions can be readily understood in the context of the existence of many competing structures with very similar energy. The interpretation of each observed phase is summarized in table 2.

Table 2. Theoretical interpretation of the stability of observed phases at room temperature, tabulated in order of appearance experimentally on increasing pressure.

Observed phase (increasing pressure)	Theoretical interpretation
Zinc-blende	Thermodynamically stable
β-tin	3D disordered, metastable to super-$Cmcm$, appears due to kinetics
$Immm$	1D disordered kinks, metastable to super-$Cmcm$, appears due to kinetics
Super-$Cmcm$	Thermodynamically stable
$Immm$	Thermodynamically stable

Acknowledgments

We would like to thank P D Hatton, R J Nelmes, D R Allan and M I McMahon for useful discussions regarding the experimentally observed structures and the conditions under which super-$Cmcm$ was formed, and S J Clark and M C Warren for discussions regarding

constant-pressure calculation. The authors would like to thank the EPSRC for support under grant No GR/K74067. AAK would like to thank the EPSRC for a studentship.

References

[1] Nelmes R J and McMahon M I 1998 *Semicond. Semimet.* **54** 145
[2] Nelmes R J, McMahon M I, Hatton P D, Crain J and Piltz R O 1993 *Phys. Rev.* B **47** 35
Nelmes R J, McMahon M I, Hatton P D, Crain J and Piltz R O 1993 *Phys. Rev.* B **48** 9949
[3] Kelsey A A, Ackland G J and Clark S J 1998 *Phys. Rev.* B **57** R2029
[4] Crain J, Ackland G J and Clark S J 1995 *Rep. Prog. Phys.* **58** 705
[5] Nelmes R J and McMahon M I 1996 *Phys. Rev. Lett.* **77** 663
[6] McMahon M I and Nelmes R J 1997 *Phys. Rev. Lett.* **78** 3697
[7] Piltz R O, Maclean J R, Clark S J, Ackland G J, Hatton P D and Crain J 1995 *Phys. Rev.* B **52** 4072
[8] Kelsey A A 1997 *PhD Thesis* University of Edinburgh
[9] Crain J, Clark S J and Ackland G J 1995 *J. Phys. Chem. Solids* **56** 495
[10] Nelmes R J and McMahon M I 1997 *Phys. Rev. Lett.* **79** 3668
[11] Guo G Y, Crain J, Blaha P and Temmerman W M 1993 *Phys. Rev.* B **47** 4841
[12] Hohenberg P and Kohn W 1964 *Phys. Rev.* **136** B864
[13] Kohn W and Sham L J 1965 *Phys. Rev.* **140** A1133
[14] Payne M C, Teter M P, Allan D C, Arias T A and Joannopoulos J D 1992 *Rev. Mod. Phys.* **64** 1045
[15] Mujica A, Needs R J and Muñoz A 1995 *Phys. Rev.* B **52** 8881
[16] Mujica A and Needs R J 1997 *Phys. Rev.* B **55** 9659
[17] Crain J, Piltz R O, Ackland G J, Clark S J, Payne M C, Milman V, Lin J S, Hatton P D and Nam Y H 1994 *Phys. Rev.* B **50** 8389
[18] Crain J, Ackland G J, Piltz R O and Hatton P D 1993 *Phys. Rev. Lett.* **70** 814
[19] Monkhorst H J and Pack J D 1976 *Phys. Rev.* B **13** 5188
[20] Vanderbilt D 1990 *Phys. Rev.* B **41** 7892
[21] Warren M C and Ackland G J 1996 *Phys. Chem. Minerals* **23** 107
[22] Bethe H 1934 *Proc. R. Soc.* A **145** 699
[23] Ackland G J 1994 *Phys. Rev.* B **50** 7389
[24] Warren M C, Ackland G J, Karki B B and Clark S J 1998 *Mineral. Mag.* **62** 585
[25] Nelmes R J and McMahon M I 1995 *Phys. Rev. Lett.* **74** 106
[26] Mezouar M, Besson J M, Syfosse G, Itie J-P, Hausermann D and Hanfland M 1996 *Phys. Status Solidi* **198** 403